ASYMMETRIC PROPAGATION OF AIRBLAST FROM BENCH BLASTING

P. Segarra[1], L.M. López[1], J.A. Sanchidrián[1], J.F. Domingo[2].

[1]Universidad Politécnica de Madrid -ETSI Minas, Ríos Rosas, 21, 28003 Madrid, Spain
[2]MAXAM Europe, Av. del Partenón, 16, 28042 Madrid, Spain

ABSTRACT

This paper investigates the propagation of airblast from quarry blasting. Peak overpressure is calculated as a function of blasting parameters (explosive mass per delay and velocity at which the detonation sequence proceeds along the bench) and polar coordinates of the point of interest (distance to the blast and azimuth with respect to the free face of the blast). The model is in the form of the product of a classical scaled distance attenuation law times a directional correction factor. The latter considers the influence of the bench face, and attenuates overpressure at the top level and amplifies it at the bottom. Such factor also accounts for the effect of the delay by amplifying the pressure in the direction of the initiation sequence if the velocity of initiation exceeds half the speed of sound and up to an initiation velocity in the range of the speed of sound. The model has been fitted to an empirical data set composed by 134 airblast records monitored in 47 blasts at two quarries. The measurements were made at distances to the blast less than 450 m. The model is statistically significant and has a determination coefficient of 0.869.

1. INTRODUCTION

Bench blasting produces environmental concerns in the form of vibrations and airblast in the surroundings of the blasting site. In addition to dynamic stresses produced in the ground by seismic waves, airblast waves will impact the walls, roof and windows of nearby structures and may induce damage on them and annoyance to their occupants (Siskind et al. 1980, Persson et al. 1994, Mohanty 1998, ISSE 1998). An accepted starting point to assess the risk of damage consists of comparing the measured peak overpressure (i.e. highest sound pressure above the atmospheric pressure) with the maximum pressure that structural elements can resist (Mohanty 1998). US Bureau of Mines recommendations (Siskind et al. 1980), worldwide used, follow that approach and set a threshold overpressure as function of the frequency response band of the transducers. Although peak overpressures from rock blasting are usually well below compliance values, the major drawback of airblast is that the induced noise may lead to buildings occupants to believe that permanent damage may have occurred (ISEE 1998).

The maximum amplitude of pressure waves in air from blasting is predicted at small pressure levels with the following formula (Persson et al. 1994):

$$P = a_0 Z^{a_1} \quad (1)$$

where a_0 and a_1 are coefficients of the model, and Z is the scaled distance defined as (Marchand 1999):

$$Z = R/M^{1/3} \quad (2)$$

or

$$Z = R/E^{1/3} \quad (3)$$

where R is the distance from the centre of the explosive source, M is the explosive mass, and E is the energy of the explosive.

Equation 1 presupposes that the detonation of different sized charges with similar geometry and of the same explosive in an isotropic medium (i.e. flat ground surface and identical atmosphere conditions) produces self- similar blast waves at identical scaled distances Z. The coefficients a_0 and a_1 are calibrated for each site by fitting Equation (1) to empirical data. They can be considered as fitting constants that lump the influence of other variables not included explicitly in Equation 1 (Hustrulid 1999). Table 1 summarizes fitting results from different work in which the scaled distances were calculated with Equation 2.

Table 1. Coefficients (a_0 and a_1) of peak overpressure attenuation function of mass-scaled distances

Source	Description of the tests	a_0	a_1
		$Pa \cdot [m \cdot kg^{-1/3}]^{-a_1}$	
Siskind et al. (1980)	Quarry blasts. Behind face	622	-0.515
	Quarry blasts. Direction of initiation	19010	-1.12
	Quarry blasts. Front of face	22182	-0.966
ISEE (1998)	Confined blasts for airblast suppression	1906	-1.1
	Blasts with average burial of the charge	19062	-1.1
Kuzu et al. (2008)	Quarry blasts in competent rocks	261.54	-0.706
	Quarry blasts in weak rocks	1833.8	-0.981
	Overburden removal	21014	-1.404
Hustrulid (1999)	Detonations in air. Unconfined	185000	-1.2

Table 1 shows that the coefficient a_0 has a large variability, nearly three orders of magnitude, which confirms that there are a number of variables that influence this coefficient. The scatter in the a_0 coefficients reported by Siskind et al. (1980) is an example of the directionality of the propagation of blast waves. In fact, the contour curves of equal overpressures from bench blasting have a shape similar to an "egg" curve, longer at the floor level and shorter at the top (Griffiths et al. 1978, Moore et al. 1993, Richards & Moore 2002, Rudenko 2002, Domingo 2007). These azimuthal variations may be reinforced in specific directions depending on the characteristics of the sequence of the blast (Siskind et al. 1980, Egorov 1996, Richards & Moore 2002). The influence of the rock type on the peak overpressure is apparent from the differences in a_0 values given by Kuzu et al (2008). The effect of charge confinement is shown by the dispersion of a_0 from ISEE data (1998), and most significantly by the high value reported by Hustrulid (1999) from shots of unconfined charges. This is consistent with other works (Siskind et al. 1980, Persson et al. 1994).

The variability of a_1 is moderate, which indicates that the influence of distance and charge is in general relatively well described by this coefficient. Atmospheric conditions also play an

important role in the attenuation of airblast; they are more relevant in the far field than in the near field (Siskind et al. 1980, Persson et al. 1994, Richards and Moore 2002).

Some of the above mentioned variables are considered together with the scaled distance to predict peak overpressures by a number of references in the literature (Moore et al. 1993, Egorov 1996, Richards & Moore 2002, Domingo 2007). This work provides a new prediction formula of the peak overpressure that accounts for asymmetrical propagation of airblast around the block to be blasted due to effect of the bench face and blast initiation.

2. DESCRIPTION OF DATA

Data arise from one single shot and 46 production blasts monitored in two quarries located in the South-East of the province of Madrid (Spain): El Alto and Monte Espartinas. A 67 % of airblast records were monitored in El Alto, and 33 % in Monte Espartinas.

El Alto belongs to Cementos Portland Valderrivas and produces 2.25 Mt/year of limestone and marl (production data from the period of study) for the cement industry. The deposit of Miocene and lacustrine origin has in the upper four to six meters an overburden of clayish-marl. The limestone pack of 12 to 19 m thick is located below the overburden. In the floor of the limestone there is a clay body, which is not mined. The ore composed by limestone and clayish marl is mined in one bench by drilling and blasting.

Monte Espartinas is some 11 km to the West of El Alto. It is owned by Saint Gobain Placo Ibérica S.A and produces 0.6 Mt/year of gypsum. The genesis of the deposit is the same than El Alto. The geology consists of a gypsum pack with a thickness of 20-30 m that underlies a vegetal soil of 0.5-1 m thick. The overburden is removed mechanically and the gypsum is mined with bench blasting techniques.

To describe the conditions in which the tests were carried out, Table 2 show the main blasting parameters. All the blasts had one free face. The number of rows was usually one. The blastholes were charged with gelatine cartridges in the bottom of the blasthole and bulk explosives above them. These were ANFO, aluminized ANFO, high density aluminized ANFO, low density ANFO and 80/20 emulsion blend. The holes were stemmed with drilling cuts. The stemming retained well detonation gasses except in 13 % of the blasts in which there was a limited stemming ejection that produced a particularly strong wave in air (i.e. stemming release pulse). The explosives were down-hole initiated with non-electric or electronic detonators. The blastsholes were delayed from the hole in one end of the block towards the other end, so the firing sequence progressed parallel to the free face of the blast. This also applies to the six blasts with multiple rows since the delay between rows was very long compared to the in-row delay. The results of the blasts in terms of toe breakage, face control, fragmentation, and muckpile characteristics are qualitatively ranked as good in all the blasts.

Dynamic overpressure in air was monitored with linear L type microphones connected to the airblast channels of recording units manufactured by Vibra-Tech and Instantel. The other channels of the units were occupied by geophones. Air overpressures were measured in a range from 0.5 to 500 Pa with a resolution of 0.25 Pa. The microphones had an operating frequency response from 2 to 250 Hz, which is adequate to measure accurately overpressures in the frequency range critical for structures and in the range of frequencies critical for human

hearing (Siskind et al. 1980, Dowding 2000). The accuracy of airblast devices is ±10 % or ±1 dB between 4 and 125 Hz, whichever is larger (ISEE 2000). The recording units were triggered when the particle velocity in the ground exceeds 0.5 mm/s. Other setups used were: sample rate of 1024 samples per second, continuous record mode of the full waveform, and automatic stop mode (the unit stops recording 2 s after the particle velocity falls below the trigger level).

Table 2. Summary of blasting and airblast data

	Mean±std.*	Range
Blasting		
Hole diameter, mm	127±24.7	89–155
Bench height, m	14.5±4.8	4.8–20.5
Blasthole length, m	15.7±4.8	5.6–23.5
Burden, m	4.4±0.7	2.9–5.5
Spacing between blastholes (S), m**	5.7±2.8	3–6.6
Mass of expl. detonated in a delay (M), kg	148±86.6	21.3–296
Energy (heat of explosion) in a delay (E), MJ	646±389	83.3–1391
Stemming length, m	3.84±1.5	1.5–6.4
Powder factor, kg/m^3**	0.40±0.07	0.17–0.51
Delay within rows, ms**	48±22	17–84
Delay between rows, ms**	161±29	100–192
Firing velocity down the face (V_I), m/s***	134±103	67–383
Airblast		
Distance to blast (R), m	136±97.5	45.1–444
Azimuth of sensor position (θ), °	162±108	2–358
Peak overpressure (P), Pa	98.2±113	6.0–482
Relative uncertainty of peak overpressure, %	3.6±4.8	0.3–19.8

* std: Standard deviation
** Data from single blasthole shot is not considered.
*** Ratio of spacing between blastholes to the delay within rows

The microphones were fitted with a foam windshield and mounted at a height of 1 m above the floor and oriented visually towards the blast. This is enough to get accurate recordings (ISEE 2009). The sensors were placed in the top level, in the bottom level or in both. When multiple microphones were used in the same blast, they were placed in different positions in El Alto and very close each other in Monte Espartinas. The reference system used to locate the measuring stations is based on that given by Griffiths et al. (1978) and shown in Figure 1; the pole is the gravity centre of the blast and the polar axis is drawn perpendicularly to the line that joins the first and last blastholes, towards the bench floor. The coordinates for each microphone position are (R, θ), where R is the distance from the pole to the microphone and θ is the angle from the polar axis towards the first hole nominally fired (in the single shot, θ is counted clockwise). The position of all sensors is shown in Figure 1, and the statistics of the polar coordinates are given in Table 2. Meteorological conditions are expected to have little influence in peak overpressures at the distances at which the sensors were placed (ISEE 1998, Richards & Moore 2002).

Peak overpressures vary between 6 to 482 Pa (see Table 2). Their uncertainties are assessed from the ratio of the standard deviation of the mean (i.e. standard deviation divided by the square root of the measurements) to the mean of the overpressures measured in the

same blast with microphones positioned right next to one another. Dispersion values of experimental errors in peak overpressure are shown in Table 2. The mean of the experimental errors is 3.6%.

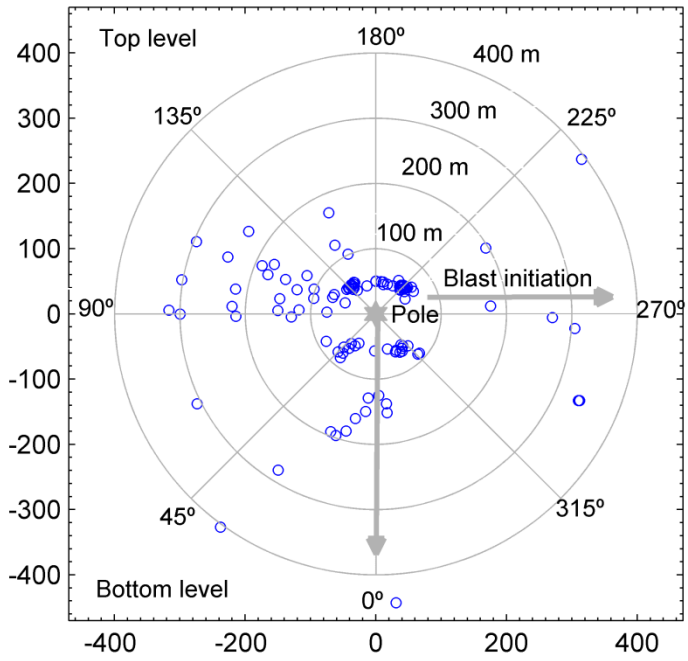

Figure 1. Reference system and sensor location (distances in m).

3. ANALYSIS AND RESULTS

Peak overpressures versus mass-scaled distance calculated with Equation 2 are plotted in Figure 2. A similar relation with the overpressure is obtained if the distance is normalized by the energy of the explosive as in Equation 3 or if the explosive mass is converted to an equivalent mass of a standard explosive. Straight mass has been used since it can be readily obtained in the field. Data in Figure 2 is split in two series as function of the level of the block to be blasted in which the sensors were placed (top and floor levels). The scatter in the data is high, and if natural logarithms are taken in Equation 1, and the resulting Equation fitted to data, the model only explains a 20.0 % of the variability of the logarithms of peak overpressure. In order to improve the prediction ability of the model, Equation 1 has been modified to account for the directional propagation by including a variable factor A:

$$P = AZ^{a_1} \tag{4}$$

A is defined as follows:

$$A = a_0 A_f A_s \tag{5}$$

where a_0 is a coefficient of the model, similar to the lead factor in Equation 1, A_f is the bench face factor that considers the influence of the azimuth of the measurement point with respect to the bench face, and A_s is the initiation sequence factor, that accounts for the effect of the blast initiation (i.e. initiation direction, delay between blastholes and relative position between blastholes along the face).

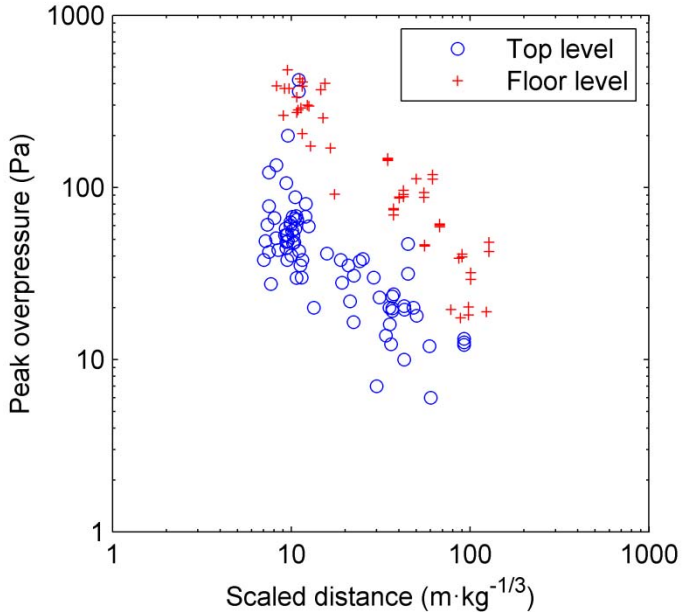

Figure 2. Peak overpressure versus mass-scaled distance.

Replacing Equation 5 into 4 leads to:

$$P = a_0 A_f A_s Z^{a_1} \tag{6}$$

The rock displacement at the bench face is the main source of airblast in properly designed blasts in which the explosive is well confined (Siskind et al. 1980). This leads, for a given scaled distance, to higher overpressures in front of the face and smaller behind it (see Figure 2). In order to account for this directional effect, the factor A_f amplifies the overpressure $a_0 Z^{a_1}$ in the bench floor level and attenuates it in the top one. Functions like: $1+a_2\cos\theta$, $1/(1-a_2\cos\theta)$ or $\exp(a_2\cos\theta)$, with a_2 a positive coefficient, could be used with similar results; the first function type was used by Griffiths et al. (1978). They are positive for all θ and are maximum at θ=0 (i.e. in front of the face) and minimum at θ=180º (i.e. behind the face). In this study, for convenience in the model fitting, the exponential form has been chosen:

$$A_f = \exp(a_2 \cos\theta) \tag{7}$$

The detonation of the explosive in each blasthole produces a pulse of air waves that may interact with the waves from nearby blastholes depending of the blast sequence and propagation path (Siskind et al. 1980, Richards and Moore 2002, Egorov 1996). If the initiation of the blast proceeds at a velocity (i.e. ratio of the spacing between blastholes to the delay within rows) close to the speed of sound, the wave generated from the detonation in a hole will reach the next hole in the sequence at about the same time that it detonates, resulting in a reinforcement of the airblast in the direction of initiation. This overlapping can also take place at subsonic velocities of initiation, with diminishing effect as initiation is slower. Siskind et al. (1980) suggest that the initiation velocity be less than half the speed of sound in order to prevent airblast reinforcement in the direction of initiation. For propagation paths in an opposite direction to the blast initiation (i.e. θ=90°, see Figure 1), the blast wave from a newly detonated hole never reaches the waves from previous ones, independently of the initiation velocity. Snell and Oltmans (1971) examined the supersonic range of initiation velocities in the direction parallel to the row of blastholes. They concluded that in such

direction, reinforcement would not occur for initiation velocities higher than 1.89 times the speed of sound. Air wave reinforcement can take place at initiation velocities in excess of that figure in directions other than the direction of blastholes initiation (i.e. directions on which the projection of the initiation velocity is approximately sonic). It should be noted, however, that highly supersonic initiation along the face is unusual in quarry blasting since it encompasses short delay times which are disfavoured for rock fragmentation performance and ground vibration, see for instance (Konya 1995). In our data the initiation velocity varies from 67 to 383 m/s (see Table 2); the latter is a fairly high value in quarry blasting.

The initiation sequence factor A_s, that accounts for the wave superposition in the direction of initiation has been defined as follows:

$$A_s = \exp(a_3 W_0) \tag{8}$$

and W_0 is defined as function of the polar angle of the position of interest and of the initiation velocity relative to the speed of sound $v_I=V_I/c$ (c is calculated from the average conditions of the tests and it is equal to 338 m/s):

$$W_0 = (1-\sin\theta)\, L(v_I) \tag{9}$$

where $L(v_I)$ is a logistic function of v_I in two parameters λ_1 and λ_2:

$$L(v_I) = \frac{1}{1+\lambda_1 \exp(\lambda_2 v_I)} \tag{10}$$

The parameters λ_1 and λ_2 are selected so that $L(v_I=0.5)= 0.01$ and $L(v_I=1)= 0.99$: $\lambda_1 = 9.703\times10^5$ and $\lambda_2 = 18.380$. Therefore W_0, and hence A_s, are maximum in the direction of initiation and for velocities of initiation around the speed of sound, and minimum in directions opposite the initiation one and at initiation velocities below half the speed of sound.

Note that if initiation velocities are much higher than the speed of sound, a bell-like or band-pass filter-type function should be required instead, with an upper cut-off value at relative initiation velocities of about 1.89, at which wave reinforcement no longer happens in the direction of initiation. In this case, other directions of reinforcement (on which the projected initiation velocity is approximately sonic) appear. Since in our data the maximum relative initiation velocity is v_I = 1.13, such upper cut-off is not required and only the direction of initiation (θ =270º) bears the maximum pressure reinforcement, as shown by the term (1-sin θ) in Equation 9.

Replacing A_f from Equation 7 and A_s from Equation 8 in Equation 6 leads to an overpressure function of three variables (Z, cos θ and W_0) with four coefficients (a_0, a_1, a_2 and a_3):

$$P = a_0 \exp(a_2 \cos\theta + a_3 W_0)\, Z^{a_1} \tag{11}$$

Taking natural logarithms in Equation 11 gives the linear function:

$$P = \log a_0 + a_2 \cos\theta + a_3 W_0 + a_1 \log Z \tag{12}$$

Equation 12 is fitted to the data set using ordinary least squares. The overpressure is given in Pascal. The scaled distance is calculated with Equation 2 as function of the explosive mass detonated in a delay. The coefficients of the regression and their main statistics are given in Table 3; the units employed are Pa for pressure and m/kg$^{1/3}$ for scaled distance. The low p-values of the coefficient estimates are strong evidence that the model is statistically valid. The

determination coefficient of the model is 0.869 and the adjusted determination coefficient R_a^2 (best indicator of the fit quality in multiple regression) is 0.866; the goodness of the fit does not change whether Equation 2 or 3 is used to calculate scaled distances. If the addend $a_3 W_0$ is discarded in Equation12 and the resulting Equation fitted to the data, R_a^2decreases to 0.776.

Table 3. Coefficients of the linear least squares regression

Coefficient	Mean	SE*	p-value**	Conf. Interval 95 %	
				Min.	Max.
log a_0	6.934	0.135	<0.0001	6.668	7.200
a_0	1027			786.8	1339
a_1	-0.953	0.042	<0.0001	-1.03	-0.870
a_2	1.24	0.050	<0.0001	1.14	1.34
a_3	1.08	0.115	<0.0001	0.855	1.31

*SE: standard error of the regression coefficients estimates.
**p-value for the t-statistic applied to the regression coefficients estimate

A plot of the measured peak overpressures versus the predicted ones is given in Figure 3; the data are differentiated as function of the blast type (single shot and production blast) and existence of stemming ejection. The regression line has a slope of one with a zero constant term. The fact that overpressures from the single blasthole shot are below the regression line is consistent with the effect of the volume of displaced rock on airblast (ISEE, 1998), since a single blasthole moves less volume of rock compared with a delayed production blast. Figure 3 also shows that the upper prediction band at a 95 % confidence level is a safe rank for blasts with stemming ejections. The residuals of the fit are also plotted in Figure 3.

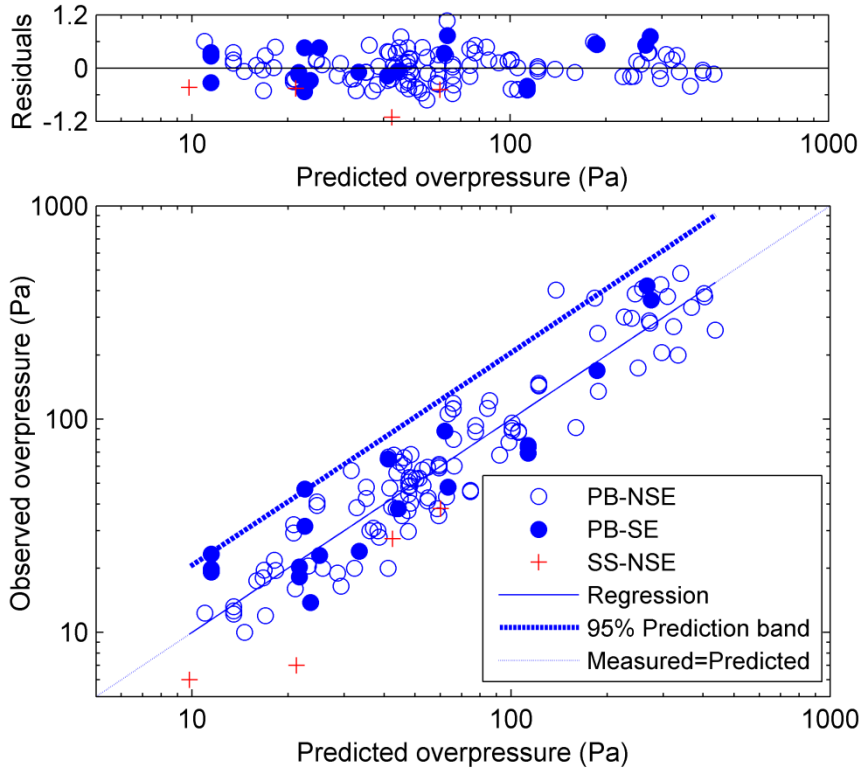

Figure 3. Measured versus predicted peak overpressures (PB: production blast, SS: single shot, NSE: no stemming ejection, and SE: stemming ejection) and residuals of the fit.

Contour maps of equal overpressure P show by inspection the main propagation features in one area (More et al. 1993, Richards and Moore 2002). Figure 4 shows, as a matter of example, the effect of the firing velocity in the propagation of blast waves. The contours of peak overpressure equal to 89.3 Pa are plotted for blasts with constant explosive mass per delay of 148 kg (mean value from the blasts monitored) and different firing velocities along the face; 89.3 Pa is the limit established by US Bureau of Mines (Siskind et al. 1980) for linear type microphones.

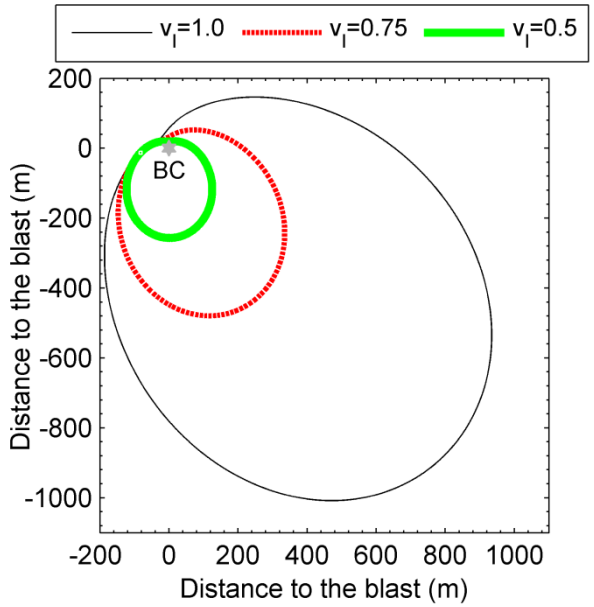

Figure 4. Contours of 89.3 Pa peak overpressure as function of the relative initiation velocity (v_I); BC is the blast centre.

Figure 5 shows a plot of the factor $A=a_0 \exp[a_2\cos\theta + a_3 W_o(\theta,v_I)]$ as function of its two variables, θ and v_I. It varies from 300.4 to 15381; the lower bound is obtained behind the face (i.e. θ=180º) for relative velocities equal to 0.5, and the largest for measurements in front of the face (i.e. θ=319º) from blasts with sonic initiation velocities. This range agrees quite well with the highest and smallest values of the coefficient a_0 for quarry blasts with confined charges given in Table 1.

The knowledge of the maximum likely peak overpressure (P_{max}) from a given blast at a certain position is useful to avoid damage and also for control purposes. Such value is estimated as the upper prediction bound of the peak overpressure at a 95 % confidence level from our model. It is given in Figure 6 as a function of the scaled distance; for each initiation velocity, lines of maximum and minimum overpressure P_{max} (corresponding to polar angles θ_{max} and θ_{min}, respectively, given in the legend of Figure 6) are plotted. As a matter of comparison, propagation laws from blasting handbooks (ISEE 1998 and Hustrulid 1999) are also represented in Figure 6.

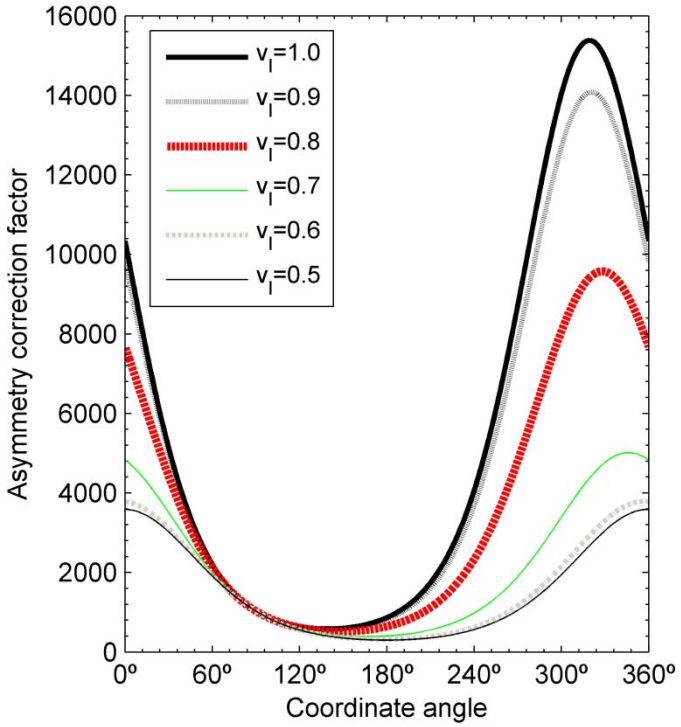

Figure 5. Asymmetry correction factor as function of the coordinate angle and relative initiation velocity (v_I)

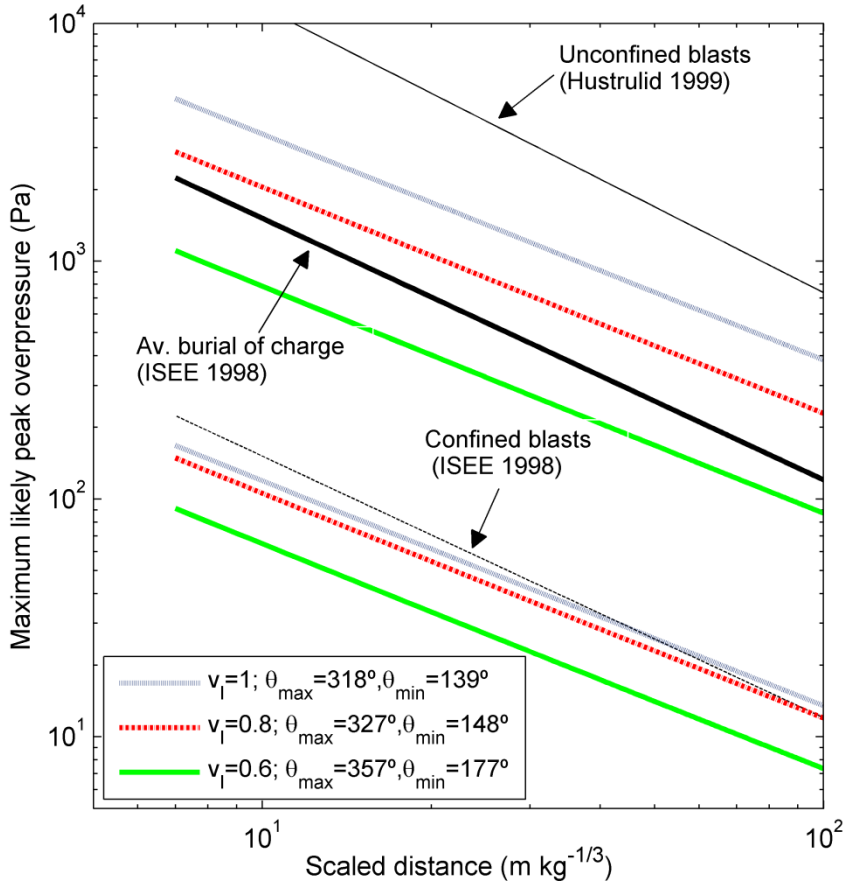

Figure 6. Maximum likely overpressures as function of the scaled distance and relative initiation velocity of the blast (v_I). Lines drawn correspond to the propagation paths at which pressure is maximum and minimum. The polar angles of these paths, θ_{max} and θ_{min} are given in the legend

4. CONCLUSIONS

Peak overpressure is a useful indicator of the damage and disturbance that airblast may produce nearby a blasting site. This work provides a model for such pressure from blasts with one free face in which the blastholes are delayed in a typical quarry blasting practice, from the hole in one end of the block towards the other end. The peak overpressure is obtained as the product of a classical scaled distance function times a directional correction factor. The scaled distance law is based on the mass of explosive per delay. The directional correction factor considers the influence of:

- Bench face: it amplifies overpressure at the bottom level (i.e. in front of the rock movement) and attenuates it at the top (i.e. behind the rock movement) through a cosine function of the polar angle or azimuth of the position of interest.
- Blast delay: It amplifies blast waves in the direction of the initiation sequence if the velocity of initiation exceeds half the sound speed, increasing the amplitude up to an initiation velocity in the range of the speed of sound.

Blasting data and airblast measurements from 134 records in 46 blasts and one single shot made in rocks with low to very low strength are used to build the model. The explosive mass in a delay varied from 21.3 to 296 kg, and the initiation velocity of the blast ranged between 67 m/s and 383 m/s. Airblast was measured with linear type microphones around the blasted blocks at distances from the blast of 45 to 444 m. The measured peak overpressures ranged from 6 to 482 Pa with a relative mean uncertainty of 3.6 %. The model explains 86.9 % of the variance in the logarithm of overpressure and is statistically meaningful. No difference in the goodness of the fit is observed when explosive energy is used instead of explosive mass.

The model is used to derive upper prediction bounds at a 95 % confidence level of peak overpressure as function of the scaled distance, initiation velocity and propagation paths. The corresponding plots can be used to assess the range of maximum blast overpressure levels expected in a particular blast design. These values are useful to evaluate whether the model can be applied in different sites.

5. ACKNOWLEDGEMENTS

Cementos Portland Valderrivas and Saint Gobain Placo Ibérica are acknowledged for their permission and support to carry out the field work. The experimental work in El Alto was partially funded by the European Union under contract no. G1RD-CT-2000-00438, “Less Fines Production in Aggregate and Industrial Minerals Industry”. The collection of data in Monte Espartinas quarry was partially funded by MAXAM, which support is gratefully acknowledged. Special recognition is due to Alberto Gómez, Javier Gutiérrez and Javier Quemada for their help and enthusiastic cooperation in the data gathering.

6. REFERENCES

Domingo, J.F., Análisis de la onda aérea producida por voladuras en banco en el campo cercano, *PhD Thesis*, Madrid: Universidad Politécnica de Madrid (2007). In Spanish.

Dowding, C.H., *Construction Vibrations*, United States: C.H. Dowding, pp.204-207 (2000).

Egorov, M.G., Blast design optimization to minimize effect of airblast, *Proc. of the 22nd Annual Conference on Explosives and Blasting Technique*, Vol. 1, Orlando, pp.286-293 (1996).

Griffiths, M.J., Oates, J.A.H & Lord, P., The propagation of sound from quarry blasting. *Journal of Sound and Vibration*, 291:358-370: (1978)

Hustrulid, W., *Blasting Principles for Open Pit Mining, Vol I– General Design Concepts*, Boca Raton: CRC Press, pp. 281-285 (1999).

ISEE, *Blasters' Handbook*, 17th Edition, Cleveland: International Society of Explosives Engineers, pp. 626-644 (1998).

ISEE, *ISEE field practice guidelines for blasting seismographs 2009 edition*. Cleveland: International Society of Explosives Engineers (2009).

ISEE, *Performance specifications for blasting seismographs*, International Society of Explosives Engineers, www.isee.org/media/pdf/2SeisPerfSpecs00.pdf (2000).

Konya, C.K., *Blast design*, Montville: Intercontinental Development Corporation (1995).

Kuzu, C., Fisne, A. & Ercelebi, S.G., Operational and geological parameters in the assessing blast induced airblast-overpressure in quarries. *Applied Acoustics* 70(3): 404-411 (2008).

Marchand, K.A., Load definition, in E.J. Conrath (Ed.), *Structural Design for Physical Security: State of the Practice*, Reston: Structural Engineering Institute, American Society of Civil Engineers, pp.2.7-2.18 (1999).

Mohanty, B., Physics of explosions hazards, in: A. Beveridge (Ed.), *Forensic Investigation of Explosions*, London: Taylor&Francis, pp. 22-32 (1998).

Moore, A.J., Evans, R. & Richards, A.B., An elliptical airblast attenuation model, *Proc. of the 4th International Symposium on Rock Fragmentation by Blasting- Fragblast 4*, Vienna, pp.247-252 (1993).

Persson, P.A., Holmberg R. & Lee, J., *Rock Blasting and Explosives Engineering*, Boca Raton: CRC Press, pp. 375-386 (1994).

Richards, A.B. & Moore, A.J., Airblast design concepts in open pit mines, *Proc. of the 7th International Symposium on Rock Fragmentation by Blasting- Fragblast 7*, Beijing, China, pp.553-561 (2002).

Rudenko D., Airblast an often overlooked cause of structural response, *Proc. of the 28th Annual Conference on Explosives and Blasting Technique*, Vol. 2, Las Vegas, pp.153-166 (2002).

Siskind, D.E., Stachura, V.J., Stagg, M.S. & Koop, J.W., *Structure response and damage produced by airblast from surface mining*, USBM Report of Investigation 8485. Twin Cities: United States Bureau of Mines (1980).

Snell, C.H. & Oltmans D.L., *A revised empirical approach to airblast prediction*, Report No. 39, Livermore: US Army Engineer Explosive Excavation Research Office, pp. 44-51 (1971).